❑   1038

DC-DC Boost Converter Design for Fast and Accurate MPPT Algorithms in Stand-Alone Photovoltaic System

Norazlan Hashim[1], Zainal Salam[2], Dalina Johari[3], Nik Fasdi Nik Ismail[4]
[1, 3, 4]Faculty of Electrical Engineering, Universiti Teknologi MARA, Malaysia
[2]Center of Electrical Energy Systems, School of Electrical Engineering, Faculty of Engineering, Universiti Teknologi Malaysia, Malaysia

Article Info	ABSTRACT
	The main components of a Stand-Alone Photovoltaic (SAPV) system consists of PV array, DC-DC converter, load and the maximum power point tracking (MPPT) control algorithm. MPPT algorithm was used for extracting maximum available power from PV module under a particular environmental condition by controlling the duty ratio of DC-DC converter. Based on maximum power transfer theorem, by changing the duty cycle, the load resistance as seen by the source is varied and matched with the internal resistance of PV module at maximum power point (MPP) so as to transfer the maximum power. Under sudden changes in solar irradiance, the selection of MPPT algorithm's sampling time (T_{S_MPPT}) is very much depends on two main components of the converter circuit namely; inductor and capacitor. As the value of these components increases, the settling time of the transient response for PV voltage and current will also increase linearly. Consequently, T_{S_MPPT} needs to be increased for accurate MPPT and therefore reduce the tracking speed. This work presents a design considerations of DC-DC Boost Converter used in SAPV system for fast and accurate MPPT algorithm. The conventional Hill Climbing (HC) algorithm has been applied to track the MPP when subjected to sudden changes in solar irradiance. By selecting the optimum value of the converter circuit components, a fast and accurate MPPT especially during sudden changes in irradiance has been realized. **

Corresponding Author:

Norazlan Hashim,
Faculty of Electrical Engineering,
Universiti Teknologi MARA,
40000 Shah Alam, Malaysia
Email: azlan4477@salam.uitm.edu.my

1. INTRODUCTION

In recent years, due to the energy crisis and environment pollution, the direct solar electricity generation using PV system become more significant. The market for solar PV system has grown rapidly over the past decade, as local governments offered various incentives to expand the solar market as well as the declining PV cost. Generally, PV system can be classified into three major categories: Stand-Alone (SA), Grid-Connected (GC) and Hybrid (H) PV system. Stand-Alone PV system are designed to operate independent of the electric utility grid, and are generally designed and sized to supply certain DC and/or AC electrical loads. In the grid-connected PV system, electricity produced from PV array are either used directly, or fed into a large electricity grid. A hybrid PV system is essentially a system that employs at least one more source, other than the PV such as wind turbines or diesel generators, to meet the electrical power demand of the loads [1].

In this work, only Stand-Alone PV system that can be utilized for any heating, cooking and water pumping applications is considered [2, 3]. In order to reduce the costs and environmental issues, the battery is not applied in these applications. One major problem with any PV system is that, the amount of electric power generated is constantly changing with weather conditions, especially solar irradiance. If the solar irradiance changes, the operating point of the PV array will shift away from its maximum power point (MPP). To overcome this problem, a Maximum Power Point Tracking (MPPT) algorithms incorporating with DC-DC converter is implemented which has led to the increase in the operation efficiency of the PV array. For SAPV system with fixed load resistance (without battery), maximum power is delivered to the load when input resistance (R_{in}) of the converter matches with the internal resistance of PV array at (R_{MPP}) based on Maximum Power Transfer Theorem. To do so, MPPT regulates the input voltage of the PV array at MPP by adjusting the duty cycle (D) of the converter.

The most popular MPPT algorithms in practice are perturb and observe (P&O), hill climbing (HC), and the incremental conductance method (INC). These conventional algorithms are widely applied due to their simplicity, ease of implementation and low cost [4]. The other conventional MPPT algorithms used in PV system are presented in [5-12]. In literature [13-17], many new improved performance of MPPT algorithms have been proposed. However, the components sizing of the different topologies of DC-DC converters have not been studied widely although this sizing affects significantly the optimum operation of the MPPT algorithms. For example, the poorly selection of the converter component sizing, especially capacitor and inductor according to the load could make MPPT operate less optimally. Under sudden step changes in irradiance, the selection of the MPPT sampling time (T_{S_MPPT}) must consider the transient response of the MPPT inputs such as PV's voltage and current, in order to avoid the delay and failure in tracking of maximum power. The three most commonly used DC-DC converters in PV system are: buck, boost and buck-boost converters. The circuit parameters and mode of operation of each topology have been discussed in [18, 19]. Boost converter has some advantages over the other converters as it is more stable and efficient [20], and hence chosen in this work.

This work focuses on the sizing effect of two DC-DC boost converter components i.e capacitor and inductor, on transient response and speed of the MPPT algorithm. Furthermore, hill climbing (HC) MPPT algorithm has been chosen to track the MPP during suddenly changing solar irradiance. Only DC-DC boost converter used in Stand-Alone PV system with fixed load resistor is considered here.

2. MPPT FOR STAND-ALONE PV SYSTEM WITH LOAD RESISTANCE

In SAPV system, the battery is crucial for power flow management if the load demands a constant voltage. However, in some applications like heating, cooking and water pumping system where the change in the load voltage will not affect the reliability of the system, the battery is not needed. In those applications, the battery is not applied to reduce cost, frequent maintenance and environmental issues caused by battery usages [2, 3]. The main objective of the system is to obtain power from the PV array as much as possible without having to regulate the output voltage and current. As per maximum power transfer theorem, maximum power is transferred to the load when equivalent load resistance referred to the input terminals of the converter (R_{in}) is match to the internal resistance of PV array at MPP (R_{MPP}). Figure 1 shows such a system.
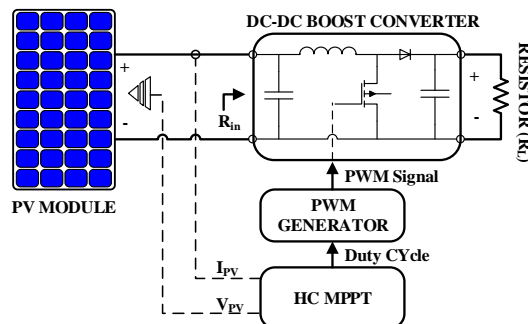

Figure 1. Block diagram of MPPT stand-alone PV systems with load resistor

2.1. PV cell modeling

In this work, the simulations model of PV system is based on MATLAB/Simulink simulator developed in [21, 22], which utilized a two-diode PV cell model as depicted in Figure 2.
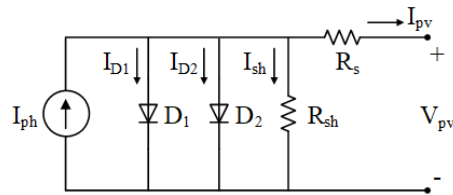

Figure 2. A Two-diode model of PV cell

It is chosen due to its superior accuracy, particularly at low irradiance level [21]. A number of series-parallel connected PV modules are used to form a PV array for a desired voltage and current level. For a string with N number of modules in series (N_{cell}), the output current of the cell is given by:

$$I = I_{PV} - I_{o1} \cdot \left[\exp\left(\frac{V + IR_s}{a_1 V_{T1}}\right) - 1 \right] - I_{o2} \cdot \left[\exp\left(\frac{V + IR_s}{a_2 V_{T2}}\right) - 1 \right] - \left(\frac{V + IR_s \times N_{cell}}{IR_p \times N_{cell}}\right) \tag{1}$$

where I_{o1} and I_{o2} are the reverse saturation currents of diode 1 (D_1) and diode 2 (D_2), respectively; V_{T1} and V_{T2} are the thermal voltages of respective diodes; a_1 and a_2 represent the diode ideality constants. In this work, 5 PV modules are connected in a single series string and provides about 299.3W as nominal maximum output power under solar irradiance of 1000W/m² at standard test condition (STC), as shown in Figure 3. The PV module is simulated using BP MSX-60 model and its specifications at STC are tabulated in Table 1.
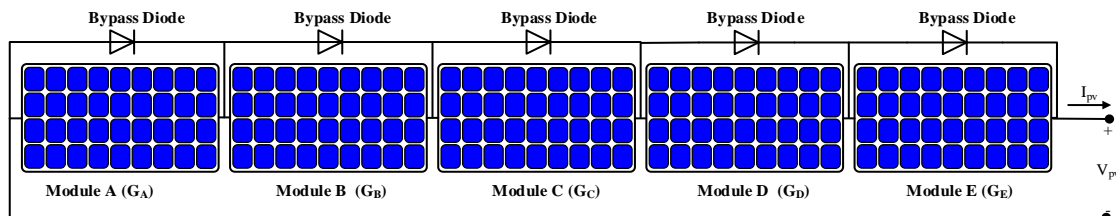

Figure 3. Five modules in series under uniform irradiance ($G_{A-E} = 1000W/m^2$)

Tabel 1. Electrical Parameters of Single BP MSX-60 Module at STC

Parameters	Values
Maximum Power (Pmax)	60 W
Voltage at Pmax (Vmpp)	17.1 V
Current at Pmax (Impp)	3.5 A
Open circuit voltage (Voc)	21.1 V
Short circuit current (Isc)	3.8 A
Temperature coefficient of Voc	-(80±10) mV/°C
Temperature coefficient of Isc	-(0.065±0.015) %/°C
Temperature coefficient of power	-(0.5±0.05) % V/°C
NOCT	47±2 °C
Operating Temperature	25 °C

In a normal condition, i.e. when the solar irradiance on the entire PV array is uniform, the power-voltage (P-V) and current-voltage (I-V) curves exhibits a single global MPP as depicted in Figure 4. To simulate the fast changing solar irradiance, two different levels of irradiance were selected, 1) highest (Point A, G=1000W/m²) and lowest (Point B, G= 300W/m²). The characteristics variation of P-V, I-V and optimal internal resistance curves of this PV array for these two irradiance levels are shown in Figure 4. It can be

seen that, the maximum power point (MPP) has changed from point A to B when the irradiance (G) level decreases from 1000W/m^2 to 300W/m^2. As a result, R_{MPP} increased from 24.6Ω to 84.4Ω which is calculated using;

$$R_{MPP} = \frac{V_{MPP}}{I_{MPP}} \tag{2}$$

It is not practical to change the load resistance manually at any moment the solar irradiance changes [23]. Therefore, MPPT algorithm has been designed to continuously adjusts the duty cycle of the converter, in order to match the input resistance to the internal resistance of PV array at MPP ($R_{in}=R_{MPP}$), and hence extracts maximum available power. At MPP, the duty cycle of the converter is calculated as [3];

$$D_{MPP} = 1 - \sqrt{\frac{R_{MPP}}{R_L}} \tag{3}$$

By assuming a lossless converter ($P_{PV}=P_{out}$), the output voltage (V_{out}) of the converter at MPP is determined as;

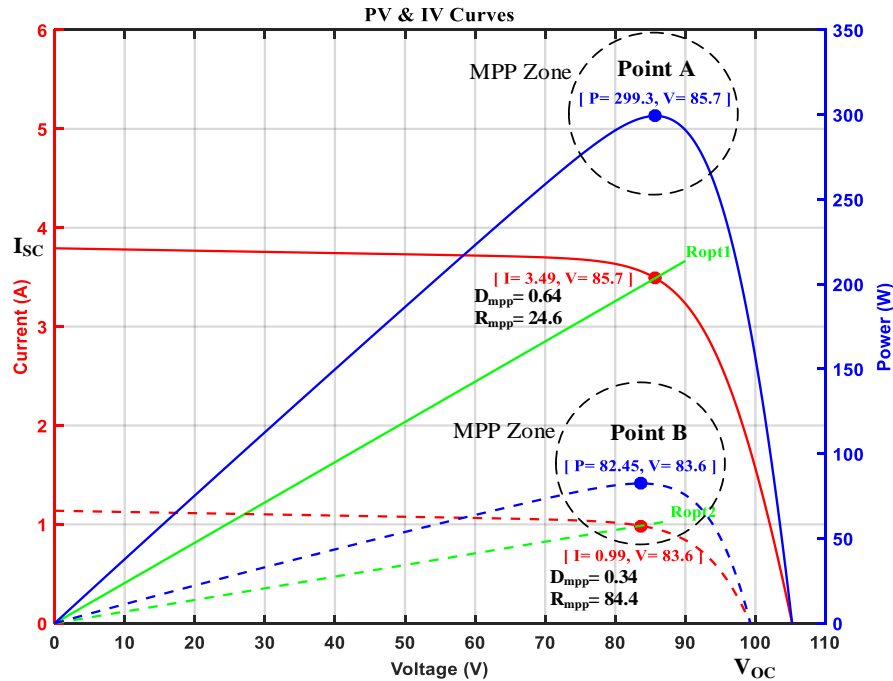$$V_{out} = \frac{V_{mpp}}{1 - D_{mpp}} \tag{4}$$

Figure 4. (a) I–V and P–V curves of PV array at two irradiance level at STC

2.2. Hill climbing (HC) MPPT algorithm

The goal of employing MPPT is to extract maximum power from PV Array at any varying atmospheric conditions especially solar irradiance changes. To do so, MPPT algorithm perturbs the duty cycle of the DC-DC converter to match the resistance of load as seen by the source (R_{in}) to the internal optimal resistance of PV Array (R_{MPP}). In this work, the conventional Hill Climbing algorithm as discussed in [4, 24-28] has been applied to track the MPP when subjected to sudden changes in solar irradiance. HC algorithm offers number of advantages: 1) it simplifies the tracking structure, 2) it reduces the computation time, and 3) no tuning effort is needed for the PI gains [28]. Practically, it can replace the expensive MPPT controller with lower cost controller while maintaining similar optimum results.

In HC, at each iteration i, the algorithm starts sensing the voltage, V(i) and current, I(i) of PV array and the corresponding power, P(i)= V(i)×I(i) is then calculated. Next, the duty cycle (D) of the converter is perturbed by an increment of duty cycle step size (D_{step}), and the resulting change of power, ΔP = P(i+1) -

P(i) is obtained. If the ΔP is positive, then perturbation is in the right direction, and more perturbation is applied in the same direction to reach the MPP. The perturbation direction is reversed if ΔP is negative, an indication that the tracking is moved away from the MPP. The flowchart of the HC algorithm is shown in Figure 5.

When solar irradiance changes, the tracking speed to reach new MPP using conventional HC algorithm depends mainly on two variables, 1) the duty cycle step size (D_{step}), and 2) the MPPT sampling time (T_{S_MPPT}) which is the time given to the MPPT to read all the inputs and solve all the calculations involved in the algorithm at each applied duty cycle (D). Large D_{step} will increase the MPP tracking speed but the power losses also increases due to the large oscillation around MPP. Small D_{step} will reduce power losses oscillation around MPP but the tracking speed will be low. Hence, the trade-off have to be made to increase the overall MPPT efficiency. In this study, D_{step} is set at 10% during exploration process and is set at 0.5% during exploitation process. Meanwhile, large T_{S_MPPT} will reduce the MPP tracking speed and vice versa.

Due to the step change in irradiance, PV voltage and current will undergo a transient response before shortly recovering to its new steady-state condition [17, 28, 29] . The settling time ($T_{Settling}$) of voltage and current depends muchly on the circuit components i.e capacitor and inductor, which will be discussed further in the next section. For accurate MPPT, T_{S_MPPT} must be designed to be greater than $T_{Settling}$ and all readings and calculations involved in algorithm must be completed within this specified period. Otherwise, the algorithm might fail to perform in the required manner.
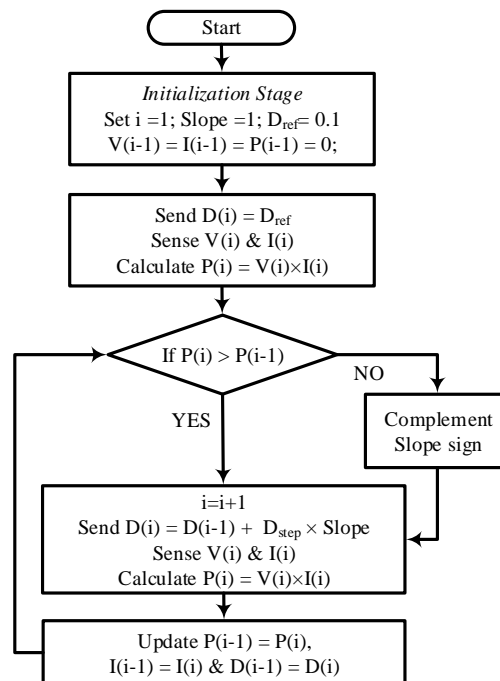

Figure 5. Flow chart of conventional HC MPPT Algorithm.

3.   DESIGN OF DC-DC BOOST CONVERTER

For Stand-Alone PV systems [30], a DC-DC boost converter is interfaced between the PV array and the load resistance as shown in Figure 1. The maximum power generated from the PV array at standard test condition (STC) is about 299.3W. The specifications of the PV module (BP-MSX60) are given in Table 1. In DC-DC boost converter, five components needs to be chosen namely, switching device, diode, inductor, capacitor and resistor. In the simulation, a standard power diode and the switching device of Power-MOSFET are chosen since there are widely used for low to medium power applications. The switching frequency is set at 20 kHz after a trade-off between the switching losses and size of inductor. Selection of other components is done as the following.

3.1. Selection of the resistor

The relationship between load resistance (R_L) of boost converter and optimal internal resistance of PV array at MPP (R_{MPP}) can be expressed as [3];

$$R_L = \frac{R_{MPP}}{\left(1 - D_{mpp}\right)^2} \tag{5}$$

Where, D_{mpp} is the converter duty cycle at maximum power point (MPP). In order to track the maximum power, the load resistance of boost converter must be greater than or equal to optimal internal resistance of PV Array at MPP ($R_L \geq R_{MPP}$), since the range of duty ratio (D) is between 0 to 1. The tracking of maximum power will fails if the above condition is not met [3]. In this work, the value of load resistance is chosen as $R_L = 200\Omega$, which is greater than the internal resistance of PV array at MPP for lowest irradiance (300W/m^2) and temperature of 25°C (STC) as in Table 2. It is a real resistance measurement for 300W rated load bank available at the lab for future hardware execution. This load bank acts as a dumping place for 299.3W power generated from PV array used in this work.

3.2. Selection of the inductor

Boost inductor value is selected based on the maximum allowable current ripple which occurs at the MPP under highest solar irradiance (1000W/m^2). The higher the inductor value, the lower is the ripple output current and vice versa. To realize a low cost converter, the lower inductor value is preferred, because inductor is the most expensive component compared to the others. In this work, the switching frequency (fs) is set at 20 kHz and the permitted amount of ripple current (ΔI) is selected as 40% of the input current [31]. Hence, the minimum value of inductor is determined as [19, 29];

$$L_{min} = \frac{V_{mpp} \times D_{mpp}}{2 \times \Delta I_{out} \times f_s} = 0.948 \text{ mH} \tag{6}$$

Here, a commercially available of 1mH, 5mH and 10mH inductors are chosen for MPPT's transient response study. For example, 1mH boost converter choke (10A, 20 kHz) is available from SMP (www.smp.de).

3.3. Selection of the capacitor

In this study, the input and output filter capacitor (C_{in} & C_{out}) are chosen to meet the voltage ripple requirement of 0.2%. An approximate expression for the required capacitance is given as [19, 29];

$$C_{min} = \frac{V_{out} \times D_{mpp}}{2 \times \Delta V_{out} \times R \times f_s} = 41.7 \text{ μF} \tag{7}$$

To study the effect of the capacitor value on the transient response of MPPT for step change in irradiance, three (3) practical capacitor values available to support the voltage of 250V are selected i.e., 47 μF, 100 μF and 220 μF. Using all the equations above, sets of data used in this work are calculated and tabulated in Table 2. PV array data under highest and lowest solar irradiance at the temperature of 25^{0}C (STC) are generated from the MATLAB/Simulink PV simulator model as proposed in [21, 22].

Table 2. PV Array and Converter characteristics in lowest and highest irradiance

Irradiance (W/m^2)	PV Array					Converter (fs = 20 kHz)				
	V_{mpp} (V)	I_{mpp} (A)	P_{mpp} (W)	R_{mpp} (Ω)	D_{mpp}	V_{out} (V)	I_{out} (A)	R_L (Ω)	L (mH)	C (uH)
1000 (Highest)	85.7	3.49	299.3	24.6	0.64	238.1	1.26	200	1	47
300 (Lowest)	83.6	0.99	82.4	84.4	0.34	126.7	0.65			

4. SIMULATION RESULTS

The simulation model of the Stand-Alone PV system with MPPT algorithm is carried out in MATLAB/Simulink (2016a) environment as in Figure 6. The PV array model is based on the simulator developed by [21, 22] and took place on 2.7GHz, 8GB RAM, Intel Core i7 laptop machine. The electrical parameters at standard test conditions (STC) of PV solar module are taken from BP MSX-60 model as tabulated in Table 1. HC algorithm has been coded in MATLAB's programming language and stored as subroutine (M-file). The simulation is carried out for 3 seconds using the solver of ode23t

(mod.stiff/Trapezoidal) with variable time step and relative tolerance of 1e-6. The MPPT sampling time (T_{S_MPPT}) is set at 0.2 second (200 ms). To study the effects of boost converter components towards MPPT transient response during sudden changes in irradiance, the simulations are divided into two cases, 1) Inductor value is fixed at 1 mH while different values of the capacitor are increased accordingly as (47μF→ 100μF→ 220μ), and 2) Capacitor value is fixed at 47μF while different values of the inductor are increased i.e (1mH → 5mH → 10mH). For both cases, sudden decrease in the irradiance is simulated from 1000W/m^2 to 300W/m^2. Meanwhile, sudden increase is simulated from 300W/m^2 to 1000W/m^2.
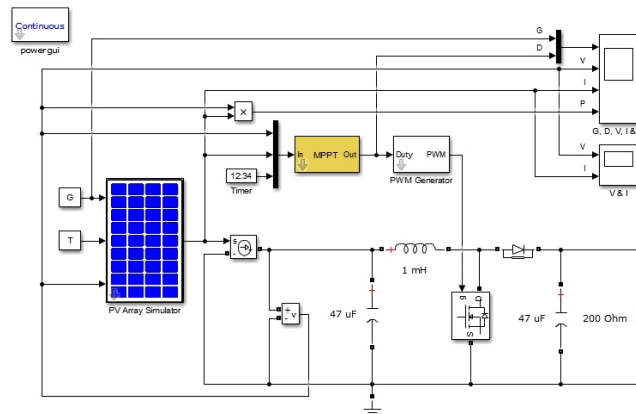

Figure 6. Simulation model of SAPV system with MPPT

4.1. Case 1 (L=1mH, C=47μF→ 100μF→ 220μF)

Figure 7 (a) shows the tracking of duty cycle, voltage, current, and power of the PV array using the conventional HC algorithm for a sudden decrease in the irradiance. Initially, the PV array is simulated at irradiance of 1000W/m^2. Hence, HC algorithm start the exploration process (D_{step}=10%) to search the MPP at point A (D=0.64, V=85.7V, I= 3.49A, P= 299.3W). When it enters the zone of MPP A, exploitation process (D_{step}=0.5%) is activated to reach the true MPP and oscillates around it as shown at 1s-2s interval in Figure 7 (a). At 2s instant, the irradiance is suddenly decreased from 1000W/m^2 to 300W/m^2. Therefore, HC starts exploring the new MPP B by reducing the duty cycle from 0.64(MPP A) to 0.54 to 0.44 and to 0.34 (MPP B). As the duty cycle decreases, the PV power will increase from 30W to 46.8W to 66.3W and to 82.3W. Once it enters the zone of MPP B, the exploitation process is used to reach true MPP which is 82.5W. In this case, the MPPT tracking speed is 800ms ($T_{S\_MPPT} \times$ 4 steps).

The tracking speed can be improved by reducing T_{S_MPPT} but it depends on the transient response of the PV voltage and current. To observe the details of transient response due to the sudden decrease in irradiance, the voltage and current waveforms are zoomed in the interval of 2s-2.2s as shown in Figure 7(b). During this interval, the duty cycle of the converter is still operated at 0.64. As seen, both voltage and current are decreased due to the decrease in irradiance. Voltage drops almost exponentially from 87.5V and after a while it stabilizes at 27.2V. Meanwhile, current undershoot from 3.49A to 0.94A before rising exponentially and stabilizes at 1.11A. By using measurement tools provided in Matlab/Simulink Scope, the settling time ($T_{settling}$) and percentage of undershoot (US)/overshoot (OS) are calculated as tabulated in Table 3. When the capacitor values increase, $T_{settling}$ also increases almost linearly from 100ms (47μF) to 190ms (100μF) and to >200ms (220μF). If 47μF capacitor is chosen for the converter, the selectable optimum value of T_{S_MPPT} is 100ms and the MPPT tracking speed will be 400ms ($T_{S\_MPPT} \times$ 4 steps). However, for 220μF capacitor the T_{S_MPPT} must be increased to >200ms in order to realize an accurate MPPT and hence decreases the MPPT tracking speed. Otherwise, the MPPT algorithm will measure the wrong values of voltage and current in which will leading to incorrect MPP detection. As for undershoot problem, all three capacitors exhibits the same condition, i.e almost 0% voltage undershoot and 15% of current undershoot. Next, the MPPT transient response under sudden increase in irradiance is investigated as in Figure 8(a-b).

The PV array is simulated at irradiance, G=300W/m^2 at the beginning of the simulation. At steady-state condition, MPPT is oscillates around MPP at point B (D=0.34, V=83.6V, I= 0.99A, P= 82.5W). At 2s instant, the irradiance is suddenly increased to 1000W/m^2. HC algorithm start searching the new MPP A by increasing the duty cycle from 0.34 to 0.64 with 0.1(10%) increment per step. Time taken to reach the zone of MPP A is 800ms (4 steps including initialise step). Figure 8 (b) shows the zoomed voltage and current

waveforms during 2s-2.2s interval. Due to sudden increase in irradiance, current overshoot to 195% (OS%) from its steady-state value for all capacitors. No overshoot observed in voltage as seen in Figure 8 (b). $T_{settling}$ for 47µF, 100µF and 220µF capacitors are 5ms, 10ms and 24ms respectively.
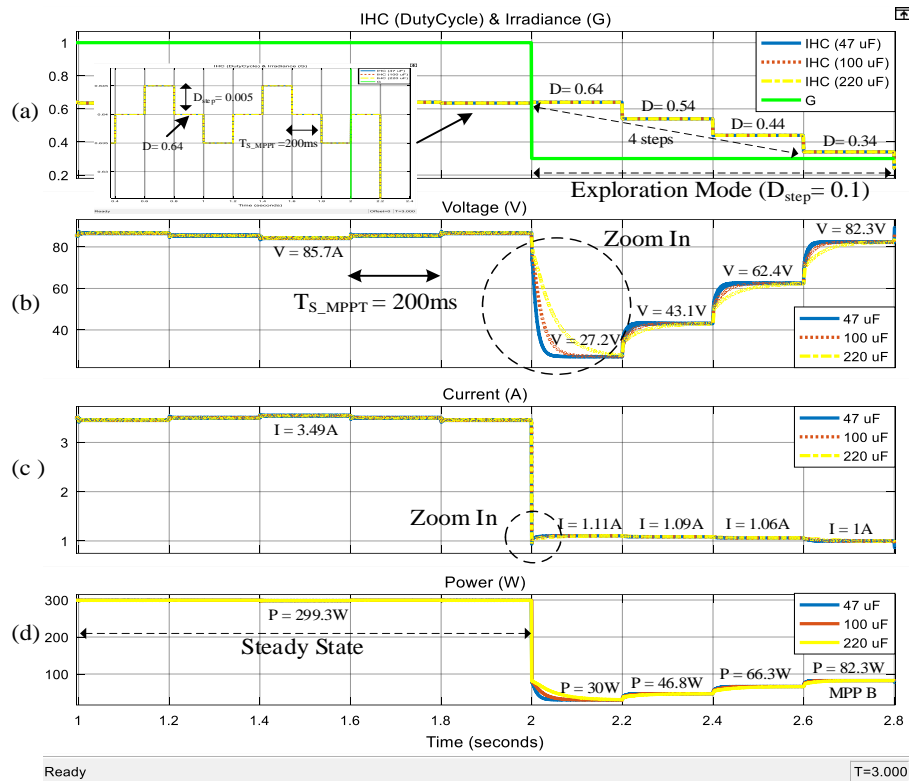

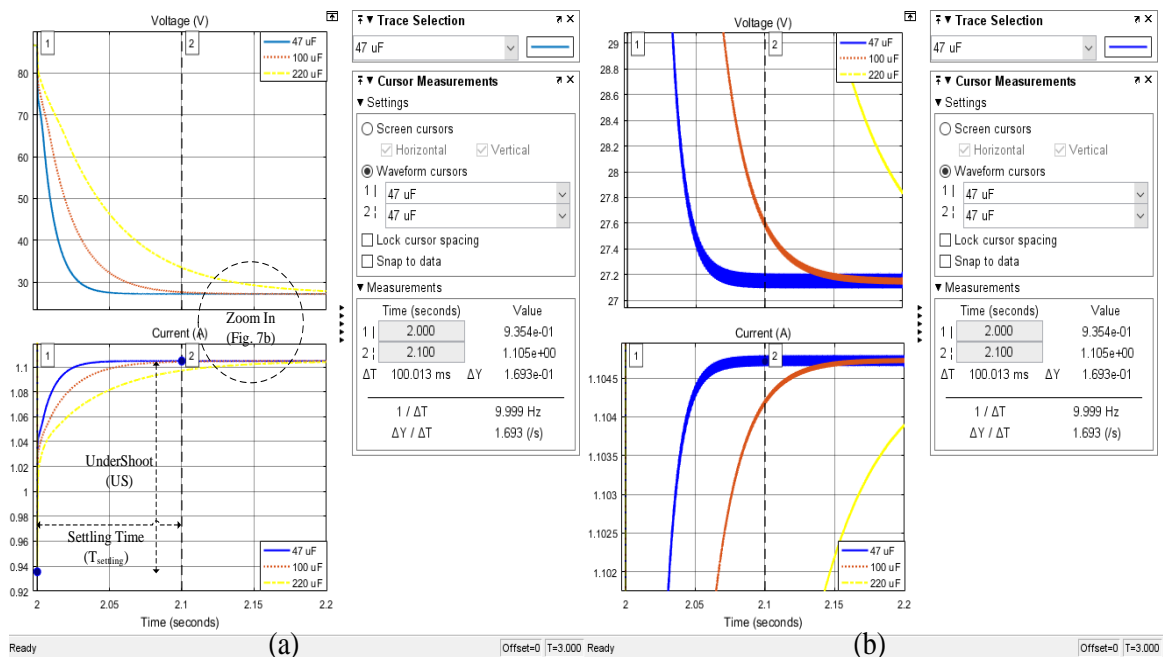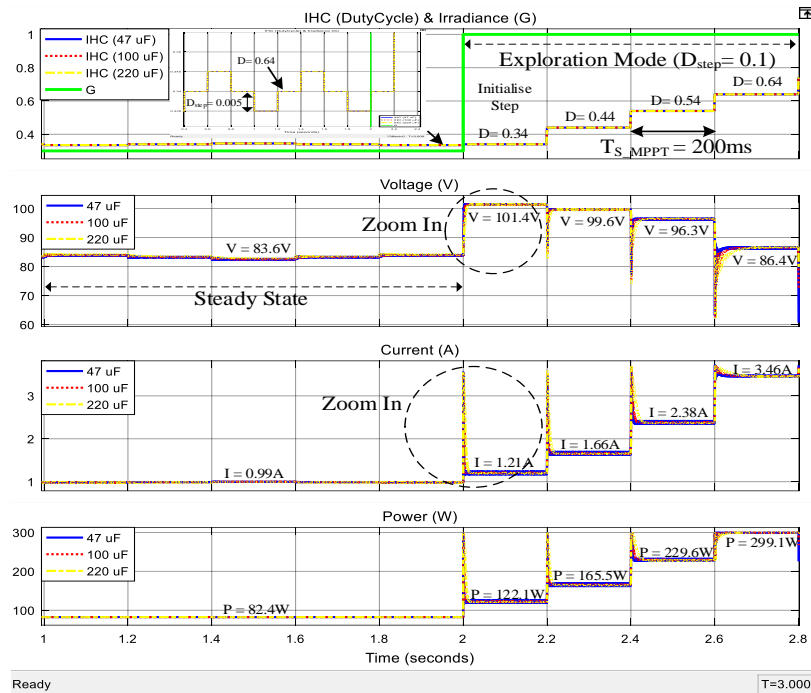Figure 7. (a) The tracking of D, V_{PV}, I_{PV}, and P_{PV} during a sudden decrease in irradiance
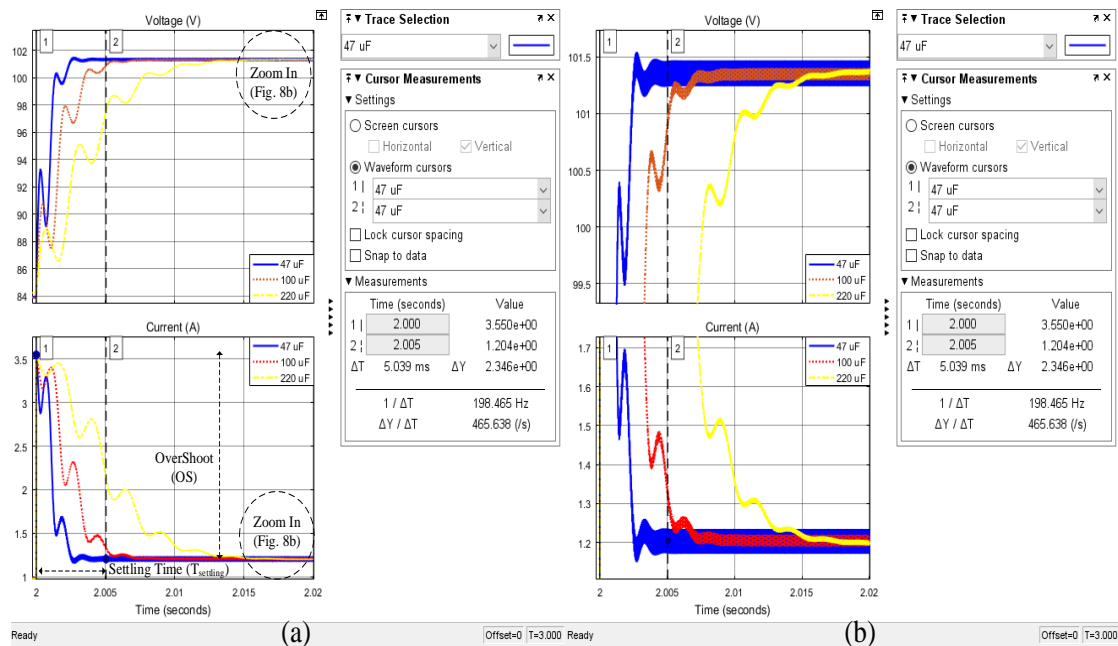

Figure 7. (b) The zoomed image of V_{PV} & I_{PV} in the interval of 2s–2.2s

Figure 8. (a) The tracking of D, V_{PV}, I_{PV}, and P_{PV} during a sudden increase in irradiance

Figure 8. (b) The zoomed image of V_{PV} & I_{PV} in the interval of 2s–2.2s

4.2. Case 2 (C=47μF, L=1mH → 5mH → 10mH)

In this case, the capacitor is fixed to its optimum value of 47μF. At 2s instant, solar irradiance is suddenly decreased/increased. The transient response of MPPT is observed by increasing the inductance value from 1mH to 5mH and to 10mH. Figure 9 (a-b) shows the MPP tracking results for sudden decreases in irradiance from 1000W/m^2 to 300W/m^2. As the inductance increase, the settling time of the waveforms will also increase. $T_{settling}$ for 1mH inductor is 100ms, while $T_{settling}$ for both 5mH and 10mH inductors exceeds the

prescribed T_{S_MPPT} value of 200ms. For fast MPPT operation, it is a wise decision to choose 1mH inductor for the converter circuit. Voltage undershoot for 1mH inductor is 0 %, for 5mH inductor is 8% and for 10mH inductor is 18%. Current undershoot is 15% for all inductors.

       Meanwhile, Figure 10 (a-b) shows the MPP tracking results for sudden increases in irradiance from 300W/m² to 1000W/m². $T_{settling}$ for 1mH inductor is 5ms, $T_{settling}$ for 5mH inductor is 20ms and $T_{settling}$ for 10mH inductor is 37ms. Voltage overshoot is between 0 to 2 %. Biggest current overshoot occurs under sudden increase in irradiance, reaching a peak of 195% from its steady state value. The overall results for both Case 1 and Case 2 are tabulated in Table 3.
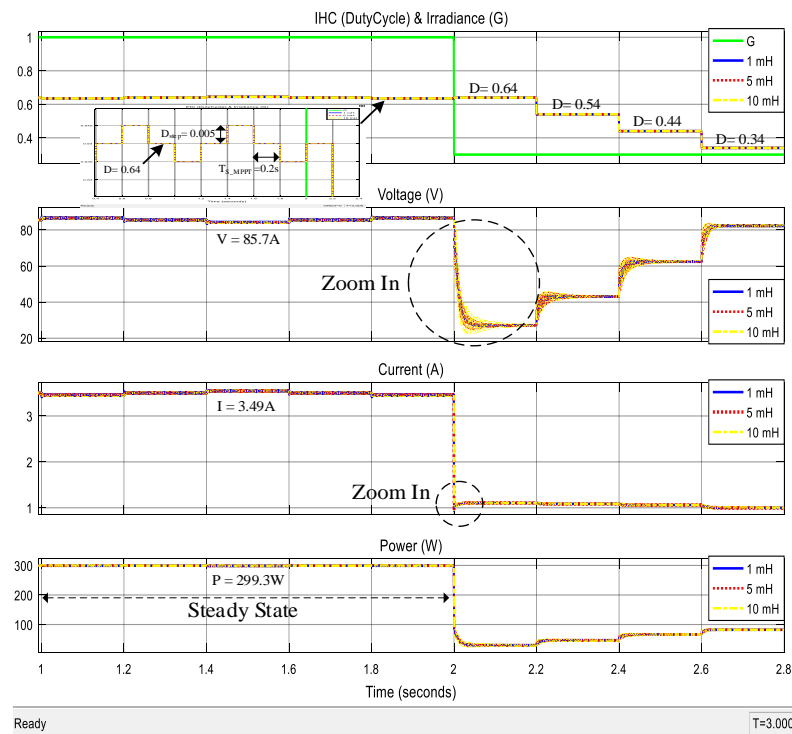

Figure 9. (a) The tracking of D, V_{PV}, I_{PV}, and P_{PV} during a sudden decrease in irradiance
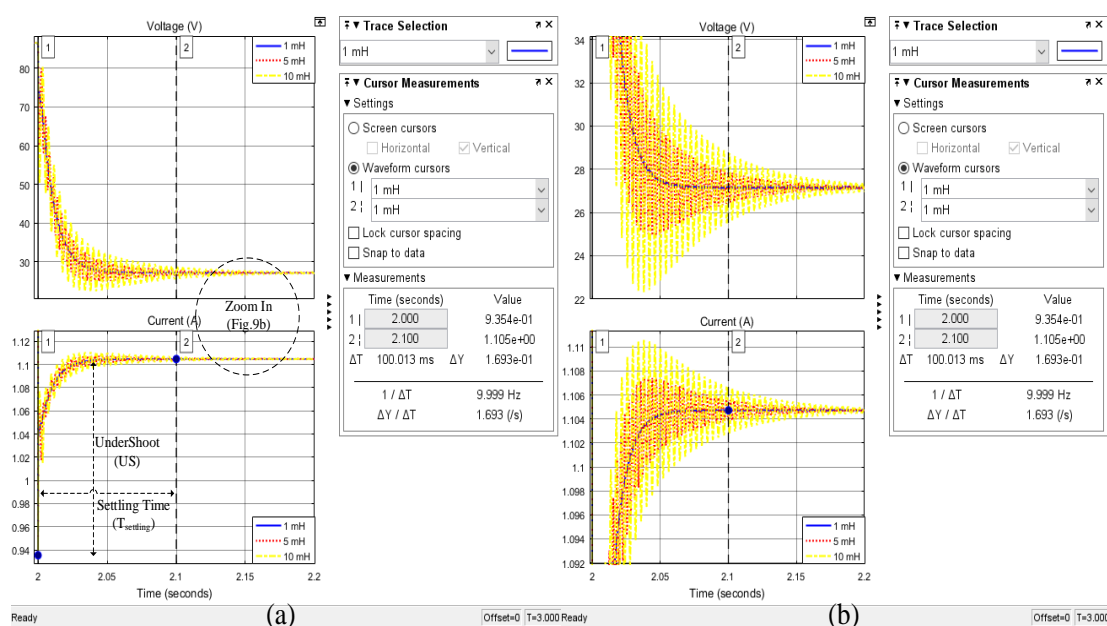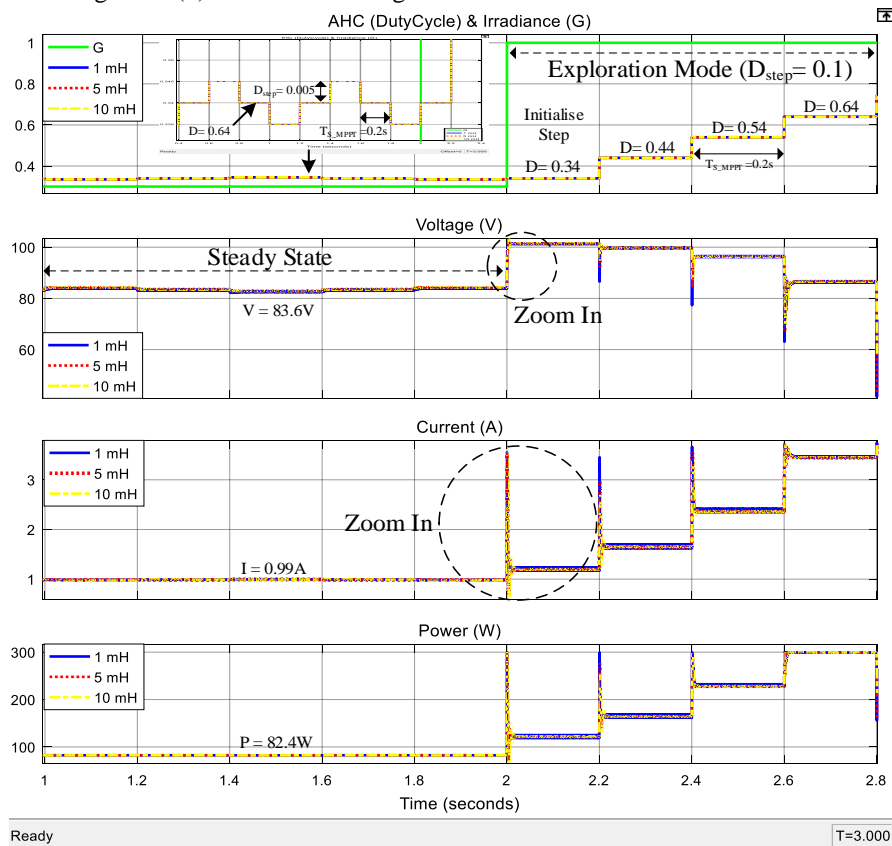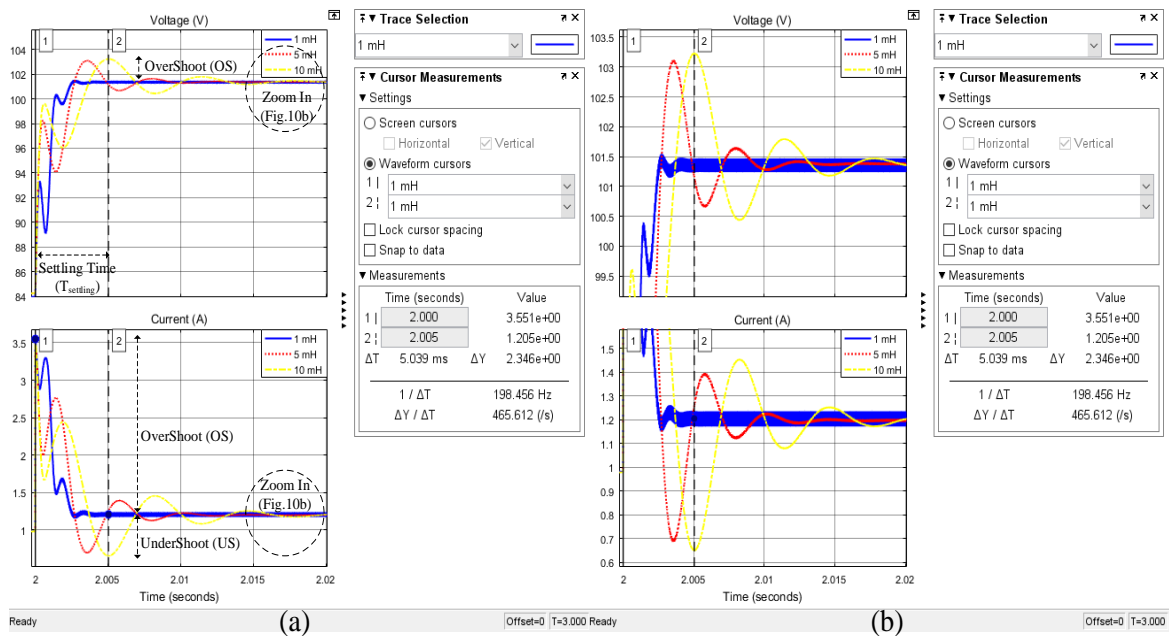
Figure 9. (b) The zoomed image of V_{PV} & I_{PV} in the interval of 2s–2.2s

Figure 10. (a) The tracking of D, V_{PV}, I_{PV}, and P_{PV} during a sudden increase in irradiance

Figure 10. (b) The zoomed image of V_{PV} & I_{PV} in the interval of 2s–2.2s

Table 3. Overall Results for Varying C&L Under Sudden Changes in Solar Irradiance

	Parameters			Sudden Decrease in Irradiance (G=1 to G=0.3, D= 0.64)		Sudden Increase in Irradiance (G=0.3 to G=1, D= 0.34)	
	C	L	V & I	Settling Time (mS)	Overshoot (OS) / Undershoot (US) (%)	Settling Time (mS)	Overshoot (OS) / Undershoot (US) (%)
CASE 1	47 µF	1 mH	V	100	0	5	0
			I		15 (US)		195 (OS)
	100 µF		V	190	0	10	0
			I		15 (US)		195 (OS)
	220 µF		V	>200	0	24	0
			I		15 (US)		195 (OS)
CASE 2	47 µF	1 mH	V	100	0	5	0
			I		15 (US)		195 (OS)
		5 mH	V	>200	8 (US)	20	2 (OS)
			I		15 (US)		195 (OS)
		10 mH	V	>200	18 (US)	37	2 (OS)
			I		15 (US)		195 (OS)

5. CONCLUSION

The effects of capacitance and inductance of DC-DC boost converter towards MPPT transient response has been demonstrated in this work. The converter is designed for 299.3W Stand-Alone PV systems connected to fixed 200Ω load resistor. As the value of capacitor and inductor increases, the settling time ($T_{settling}$) of voltage and current waveforms will also increase and vice versa. In order to improve the tracking speed and the accuracy of the MPPT under suddenly (step) changes in irradiance, the value of capacitor and inductor must be selected as low as possible while maintaining the permissible ripple limit. T_{S_MPPT} must be equal to or greater than the maximum $T_{settling}$ of the circuit. Otherwise, the wrong MPP might be tracked. In this work, the optimum value of capacitor and inductor are chosen as 47µF and 1mH respectively. The optimum value of T_{S_MPPT} is found to be 100ms. Due to the sudden changes in irradiance, MPPT takes 400ms to reach the new MPP zone. Meanwhile, the biggest current overshoot occurs during suddenly increase in irradiance from 300W/m^2 to 1000W/m^2 i.e 195%. Although, overshoot/undershoot does not directly affects the tracking speed, but it may increase the noise margin and damage the internal FET of the gate IC. By selecting optimum circuit parameter values, a fast and accurate MPPT especially during sudden changes in irradiance is realized.

ACKNOWLEDGEMENTS

REFERENCES

[1] C. S. Solanki, *Solar photovoltaics: fundamentals, technologies and applications*. PHI Learning Pvt. Ltd., 2015.
[2] A. Oi, M. Anwari, and M. Taufik, "Modeling and simulation of photovoltaic water pumping system," in *Modelling & Simulation, 2009. AMS'09. Third Asia International Conference on*, 2009, pp. 497-502: IEEE.
[3] B. Nayak, A. Mohapatra, and K. B. Mohanty, "Selection criteria of dc-dc converter and control variable for MPPT of PV system utilized in heating and cooking applications," *Cogent Engineering,* vol. 4, no. 1, p. 1363357, 2017.
[4] H. Rezk and A. M. Eltamaly, "A comprehensive comparison of different MPPT techniques for photovoltaic systems," *Solar energy,* vol. 112, pp. 1-11, 2015.
[5] J. Ahmed and Z. Salam, "A critical evaluation on maximum power point tracking methods for partial shading in PV systems," *Renewable and Sustainable Energy Reviews,* vol. 47, pp. 933-953, 2015.
[6] T. Esram and P. L. Chapman, "Comparison of Photovoltaic Array Maximum Power Point Tracking Techniques," *Energy Conversion, IEEE Transactions on,* vol. 22, no. 2, pp. 439-449, 2007.
[7] R. Faranda, S. Leva, and V. Maugeri, "MPPT techniques for PV Systems: Energetic and cost comparison," in *Power and Energy Society General Meeting - Conversion and Delivery of Electrical Energy in the 21st Century, 2008 IEEE*, 2008, pp. 1-6.
[8] D. Hohm and M. E. Ropp, "Comparative study of maximum power point tracking algorithms," *Progress in photovoltaics: Research and Applications,* vol. 11, no. 1, pp. 47-62, 2003.
[9] K. Ishaque and Z. Salam, "A review of maximum power point tracking techniques of PV system for uniform insolation and partial shading condition," *Renewable and Sustainable Energy Reviews,* vol. 19, no. 0, pp. 475-488, 3// 2013.
[10] K. Ishaque, Z. Salam, and G. Lauss, "The performance of perturb and observe and incremental conductance maximum power point tracking method under dynamic weather conditions," *Applied Energy,* vol. 119, pp. 228-236, 2014.

[11] J. P. Ram, T. S. Babu, and N. Rajasekar, "A comprehensive review on solar PV maximum power point tracking techniques," *Renewable and Sustainable Energy Reviews,* vol. 67, pp. 826-847, 2017.

[12] M. Tajuddin, M. Arif, S. Ayob, and Z. Salam, "Perturbative methods for maximum power point tracking (MPPT) of photovoltaic (PV) systems: a review," *International Journal of Energy Research,* vol. 39, no. 9, pp. 1153-1178, 2015.

[13] J. Ahmed and Z. Salam, "An improved perturb and observe (P&O) maximum power point tracking (MPPT) algorithm for higher efficiency," *Applied Energy,* vol. 150, pp. 97-108, 2015.

[14] J. Ahmed and Z. Salam, "A modified P&O maximum power point tracking method with reduced steady-state oscillation and improved tracking efficiency," *IEEE Transactions on Sustainable Energy,* vol. 7, no. 4, pp. 1506-1515, 2016.

[15] J. Ahmed and Z. Salam, "An Enhanced Adaptive P&O MPPT for Fast and Efficient Tracking Under Varying Environmental Conditions," *IEEE Transactions on Sustainable Energy,* 2018.

[16] R. H. Ashique, Z. Salam, and J. Ahmed, "An adaptive P&O MPPT using a sectionalized piece-wise linear PV curve," in *Energy Conversion (CENCON), 2015 IEEE Conference on*, 2015, pp. 474-479: IEEE.

[17] K. Ishaque and Z. Salam, "A deterministic particle swarm optimization maximum power point tracker for photovoltaic system under partial shading condition," *IEEE transactions on industrial electronics,* vol. 60, no. 8, pp. 3195-3206, 2013.

[18] S. Kolsi, H. Samet, and M. B. Amar, "Design Analysis of DC-DC converters connected to a photovoltaic generator and controlled by MPPT for Optimal energy transfer throughout a clear day," *Journal of Power and Energy Engineering,* vol. 2, no. 01, p. 27, 2014.

[19] D. W. Hart, *Power Electronics*. Tata McGraw-Hill, 2011.

[20] A. Hayat, A. Faisal, M. Y. Javed, M. Hasseb, and R. A. Rana, "Effects of input capacitor (cin) of boost converter for photovoltaic system," in *Computing, Electronic and Electrical Engineering (ICE Cube), 2016 International Conference on*, 2016, pp. 68-73: IEEE.

[21] K. Ishaque, Z. Salam, and Syafaruddin, "A comprehensive MATLAB Simulink PV system simulator with partial shading capability based on two-diode model," *Solar Energy,* vol. 85, no. 9, pp. 2217-2227, 9// 2011.

[22] K. Ishaque, Z. Salam, and H. Taheri, "Simple, fast and accurate two-diode model for photovoltaic modules," *Solar Energy Materials and Solar Cells,* vol. 95, no. 2, pp. 586-594, 2// 2011.

[23] S. S. Mohammed and D. Devaraj, "Fuzzy based maximum power point tracking controller for stand-alone photovoltaic system using MATLAB/simulink," *Int. J. of Appl. Eng. Research,* vol. 10, no. 55, pp. 3101-3106, 2015.

[24] F. Liu, Y. Kang, Y. Zhang, and S. Duan, "Comparison of P&O and hill climbing MPPT methods for grid-connected PV converter," in *Industrial Electronics and Applications, 2008. ICIEA 2008. 3rd IEEE Conference on*, 2008, pp. 804-807: IEEE.

[25] T. Esram and P. L. Chapman, "Comparison of photovoltaic array maximum power point tracking techniques," *IEEE Transactions on energy conversion,* vol. 22, no. 2, pp. 439-449, 2007.

[26] N. Femia, G. Petrone, G. Spagnuolo, and M. Vitelli, "Optimization of perturb and observe maximum power point tracking method," *IEEE transactions on power electronics,* vol. 20, no. 4, pp. 963-973, 2005.

[27] N. Fermia, D. Granozio, G. Petrone, and M. Vitelli, "Predictive & adaptive MPPT perturb and observe method," *IEEE Transactions on Aerospace and Electronic Systems,* vol. 43, no. 3, 2007.

[28] K. Ishaque and Z. Salam, "A review of maximum power point tracking techniques of PV system for uniform insolation and partial shading condition," *Renewable and Sustainable Energy Reviews,* vol. 19, pp. 475-488, 2013.

[29] S. K. Kollimalla and M. K. Mishra, "A novel adaptive P&O MPPT algorithm considering sudden changes in the irradiance," *IEEE Transactions on Energy conversion,* vol. 29, no. 3, pp. 602-610, 2014.

[30] N. Hashim, Z. Salam, and S. Ayob, "Maximum power point tracking for stand-alone photovoltaic system using evolutionary programming," in *Power Engineering and Optimization Conference (PEOCO), 2014 IEEE 8th International*, 2014, pp. 7-12: IEEE.

[31] T. Instruments, "Basic calculation of a boost converter's Power Stage," *Application Report* SLVA327B, 2009.